Ersch. in: International Journal of Quantum Chemistry ; 113 (2013), 13. - S. 1787-1793

http://dx.doi.org/10.1002/qua.24401

Small Changes—Huge Influences: NMR Chemical Shifts of Ni(II) Complexes with Polar Substrates

Andrea Frank,[a] Andreas Berkefeld,[b] Matthias Drexler,[a] Heiko M. Möller,[a] and Thomas E. Exner*[a,c]

Neutral Ni(II) complexes have been shown to be highly valuable as robust and versatile catalysts in olefin polymerization. But they show reduced reactivity when the polar monomers methyl acrylate and vinyl acetate are incorporated. To get further insight into this behavior, NMR chemical shift calculations were performed on the system [(N,O) Ni (H) (PMe3)] 1 (N,O = κ^2-N,O-{2,6-(3,5-(F3C)2C6H3)2C6H3) N=C(H)-3,5-I2-2-O-C6H2}). The chemical shifts show reasonable agreement with experiment but are also extremely influenced by geometrical features of the complex as well as the inserted substrate. The first prominent feature, the low-field shift of the $C_{carbonyl}$ in the incorporated monomer, can only be reproduced when it is in close proximity to the Ni and in this way hinders the attack of a new monomer. Second, the almost 100 ppm difference in the chemical shift of the carbon of the two substrates directly bound to Ni can be reasoned by the different directionality of polarization as disclosed by natural bond orbital (NBO) analysis.

Introduction

Their comparatively low oxophilicity has made late transition-metals attractive candidates in the search for single site catalyst for olefin polymerization[1–3,45] that are highly reactive but also tolerant toward polar functional groups and ubiquitous impurities such as water.[4–6] Neutral alkyl complexes of Ni stabilized by κ^2-O,N-salicylaldiminato ligands are of particular interest in this context in light of their remarkable functional group tolerance.[7] Particular members of this family of compounds were shown to polymerize 1-olefins in aqueous media to produce surfactant stabilized high-molecular weight polyolefin latices.[8–10] Contrasting this outstanding performance, these compounds fail to mediate the insertion polymerization of commercially relevant monomers such as methyl acrylate (MA) and vinyl acetate (VA).[11]

In the context of a mechanistic study of the putative Ni species relevant in the polymerization of functional group containing monomers, the reactivity of the precursor complex [(N,O) Ni (H) (PMe_3)] **1** (N,O = κ^2-N,O-{2,6-(3,5-$(F_3C)_2C_6H_3)_2C_6H_3$)-N=C(H)-3,5-I_2-2- *O*-C_6H_2}, see Fig. 1) was studied toward MA and VA.[12] These studies concluded that MA insertion into the Ni(II)-hydride bond of **1** occurs in a 2,1-fashion yielding the functionalized Ni(II)-alkyl complex [(N,O) Ni ($C_\alpha H(CH_3)C_\beta(O)OCH_3$) ($PMe_3$)] **4** (numbering of compounds according to Ref. [12] as shown in Fig. 2). VA shows a significantly different reactivity. Exposure of **1** to VA initially affords the kinetic 1,2-insertion product [(N,O) Ni ($CH_2CH_2OC(O)CH_3$) (PMe_3)] **5** which rearranges into the thermodynamic 2,1-insertion product [(N,O) Ni ($CH(CH_3)OC(O)CH_3$) (PMe_3)] **6** (Fig. 3). Solution structural assignments of **4**, **5**, and **6** were additionally in good agreement with geometry optimizations using density functional theory (DFT).

We will report here on ^{13}C NMR chemical shift calculations to further validate the structures of the 2,1-insertation products proposed in Berkefeld et al.[12] These studies were motivated since experimentally observed chemical shifts show unusual values and remarkable variance despite the chemical similarity of the complexes: (1) A significant shift of the carbonyl resonance by 15 ppm to lower field (186 ppm) is seen in both complexes. This was reasoned by an interaction between Ni(II) and the carbonyl oxygen atom resulting in the formation of 4- and 5-membered chelate species in **4** and **6**, respectively. Structurally related examples of Ni and Pd alkyl chelate complexes are well known and fully characterized.[13,14] (2) For the carbon atoms directly bound to Ni(II) ^{13}C NMR resonances at 4.4 and 96 ppm were measured in **4** and **6**, respectively. The calculations performed here reproduce these results in part but also show the extreme influence of small structural changes on the calculated NMR chemical shift values.

[a] *A. Frank, M. Drexler, H. M. Möller, T. E. Exner*
Department of Chemistry and Zukunftskolleg, University of Konstanz, 78457 Konstanz, Germany

[b] *A. Berkefeld*
Department of Chemistry, Technische Universität Berlin, Straße des 17.Juni 135, 10623 Berlin, Germany

[c] *T. E. Exner*
Theoretical Medicinal Chemistry and Biophysics, Institute of Pharmacy, University of Tübingen, Auf der Morgenstelle 8, 72076 Tübingen, Germany
E mail: thomas.exner@uni konstanz.de

Contract grant sponsor: Juniorprofessoren Programm of the state Baden Württemberg.
Contract grant sponsor: German Research Foundation; contract grant number: EX15/17 1.
Contract grant sponsor: Zukunftskolleg of the Universität Konstanz.
Contract grant sponsor: Konstanz Research School Chemical Biology (KoRS CB).

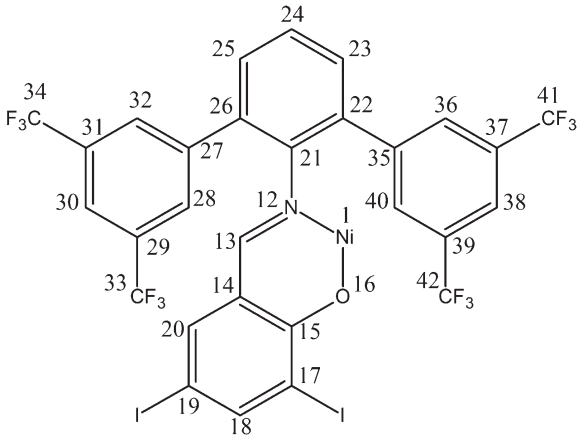

Figure 1. Numbering scheme for neutral Ni(II) complexes [(N,O) Ni (H) (PMe_3)] **1** (N,O = κ^2 N,O 2,6 (3,5 $(F_3C)_2C_6H_3)_2C_6H_3$) N=C(H) 3,5 I_2 2 *O* C_6H_2, R = F): cis positioned PMe_3 ligand fills the 3rd coordination site at Ni(II).

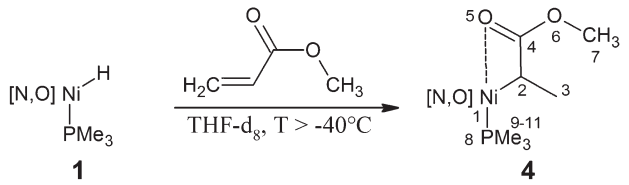

Figure 2. MA insertion into the Ni(II) hydride bond of **1** yielding directly the 2,1 insertion product of the functionalized Ni(II) alkyl complex [(N,O) Ni ($C_\alpha H(CH_3)C_\beta(O)OCH_3$) ($PMe_3$)] **4**.

Materials and Methods

Our new work is based on the previous reported geometry optimization.[12] Thus, we will first give a short summary of these. Then, our new calculations will be described.

Crystallographic data of the complex [(N,O) Ni (Cl) (PMe_3)] were used to model the complexes **4**, **5**, and **6**. These were then first optimized with the MM+ force field using the Hyperchem software.[15] Stable structures were identified by geometry scans calculating stationary points on the potential energy surface for Ni O carbonyl distances between 3.8 and 2.2 Å for **4** and between 4.8 and 1.9 Å for **6** in steps of 0.1 Å. In the case of **5**, distances between 5.5 and 2.2 Å with a step size of 0.2 Å were used. To localize the true optima, free geometry optimizations were started from the minima in the scans without restraints on the Ni O distance. All these calculations were performed using DFT with the BP86 functional and the LACVP* basis set with the Jaguar program package.[16] For **4**, a distance of 3.1 Å was found slightly below the sum of the van-der-Waals radii of Ni and oxygen (3.15 Å). For compound **5**, the product of migratory 1,2-insertion of VA, two minima are found at 2.8 and 4.9 Å with the latter minimum having the lower energy. In the 2-1-insertion complex **6**, the only minimum is located at 2.8 Å well below the sum of the van-der-Waals radii.

Here, we present new theoretical investigations based on ^{13}C chemical shift and natural bond orbital (NBO) calculations with the Gaussian03 program package[17] focusing on the two 2,1-insertion products **4** and **6**. DFT with the BP86[18] as well as the B3LYP[19,20] functionals was chosen as level of theory. The 6″ 31g(d)[21,22] as well as the 6″ 311g(d)[23,24] basis set (for all atoms except Ni(II)) were used if not stated otherwise. Solvent and finite-temperature effects were neglected. Because of the differences in the programs (Jaguar and Gaussian03) as well as the theories and basis sets used, the structures taken from the previous study were once again geometry optimized and vibrational frequencies were calculated to verify that stable minimum structures were reached. The resulting conformations were then taken for the ^{13}C NMR chemical shift calculations based on the Gauge Including Atomic Orbital method.[25–29] Besides the calculations on these locally optimized structures, some geometric features were varied by relaxed potential energy scans to see their influence on the chemical shifts.

NBO calculations were performed to study the extremely different chemical shift values of corresponding nuclei in the two complexes. NBO version 5.0[30] was applied in all calculations. Since such analyses are very complicated and hardly interpretable for large systems, smaller parts cut out of the complete complexes were taken. This way, decomposition of the many-electron molecular wave function into localized electron-pair bonding and lone-pair units allowed to quantify the electron displacement between different parts of the molecules explaining the different electron density and orbital contributions at the nuclear positions resulting in the chemical shift variation. Because of their relatively small sizes, Møller–Plesset second-order perturbation theory (MP2)[31–35] calculations were performed on these fragments to corroborate the DFT results.

Results and Discussions

Starting from the structures proposed by Berkefeld et al.[12] when changing the distance between Ni and $O_{carbonyl}$, the

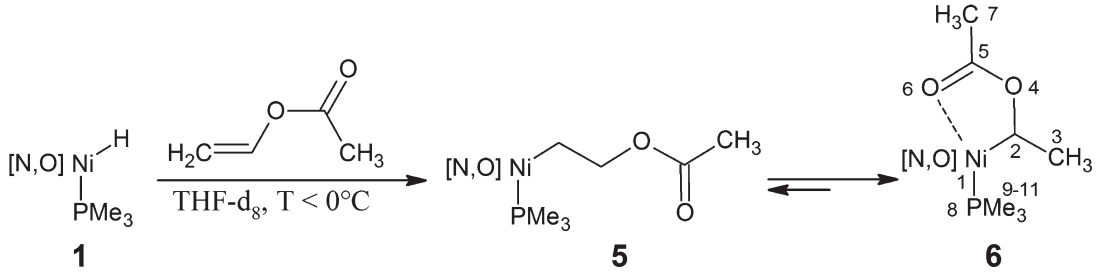

Figure 3. VA insertion into the Ni(II) hydride bond of **1** yielding first the kinetic 1,2 insertion and finally the thermodynamic 2,1 insertion product of the functionalized Ni(II) alkyl complex [(N,O) Ni ($CH(CH_3)OC(O)CH_3$) (PMe_3)] **6**.

Table 1. Distances from Ni(II) to the atoms of the α methoxycarbonyl ethyl ligand in **4**: The corresponding atoms are printed in italics and the atom numbers according to Figure 2 are given in brackets. For comparison, the values from Berkefeld et al.[12] are also listed.

R=methyl acrylate	Distance from Ni(II) to ...				From Ref. [12]
Basis set	6 311G(d)		6 31G(d)		LACVP*
Atoms\Functional	B3LYP	BP86	B3LYP	BP86	BP86
C$HCH_3C(O)OCH_3$ (2)	1.980	1.977	1.963	1.952	1.998
CH***C***$H_3C(O)OCH_3$ (3)	3.055	3.038	3.063	3.042	3.055
$CHCH_3$***C***$(O)OCH_3$ (4)	2.826	2.861	2.792	2.804	2.847
$CHCH_3C(O)O$***C***H_3 (7)	5.091	5.156	5.055	5.104	5.119
P$(CH_3)_3$ (8)	2.241	2.201	2.226	2.189	2.227
$CHCH_3C($***O***$)OCH_3$ (5)	3.095	3.145	3.052	3.055	3.130
$CHCH_3C(O)$***O***CH_3 (6)	3.971	4.026	3.948	3.995	3.999

complexes were again energetically minimized using four different functional/basis set combinations as described above. The most relevant geometrical features of the optimized complex structures are given in Tables 1 and 2. These structures will be called *optimized starting structure* in the following. Most of the values show only minor variation with respect to the functional/basis set used and are comparable to the one published before. Only the Ni $O_{carbonyl}$ (atom no. 1 and 6 in Fig. 3) distance in **6** increases from 2.8 to 3.0 Å when using the larger basis set. This seems to be a large disagreement between the smaller and larger basis set. But the minimum in this complex is shallow with respect to the Ni O distance as shown in the distance scans,[12] so that here small changes in energy can lead to large structural changes and the 0.2 Å have to be considered well within the error bar of the theoretical method. Additionally, the larger basis set predicts the distance still to be smaller than the sum of the van-der-Waals radii even if not that pronounced. Thus, the circumstantial evidence from the NMR data that there is an interaction between Ni and the carboxyl group leading to a five-fold coordination of Ni is still supported.

Table 2. Distances from Ni(II) to the atoms of the α acetoxy ethyl ligand in **6**: The corresponding atoms are printed in italics and the atom numbers according to Figure 3 are given in brackets. For comparison, the values from Berkefeld et al.[12] are also listed.

R=vinyl acetate	Distance from Ni(II) to ...				From Ref. [12]
Basis set	6 311G(d)		6 31G(d)		LACVP*
Atoms\Functional	B3LYP	BP86	B3LYP	BP86	BP86
C$HCH_3O(O)CCH_3$ (2)	1.930	1.926	1.916	1.907	1.945
CH***C***$H_3O(O)CCH_3$ (3)	3.023	3.009	3.032	3.017	3.016
$CHCH_3O(O)$***C***CH_3 (5)	3.269	3.288	3.148	3.144	3.172
$CHCH_3O(O)C$***C***H_3 (7)	4.695	4.724	4.610	4.618	4.631
P$(CH_3)_3$ (8)	2.238	2.197	2.224	2.184	2.224
$CHCH_3$***O***$(O)CCH_3$ (4)	2.852	2.868	2.834	2.843	2.864
$CHCH_3O($***O***$)CCH_3$ (6)	3.035	3.043	2.813	2.784	2.780

One additional argument for the Ni O interaction was the ^{13}C NMR chemical shift of the carbonyl carbon, which is shifted to lower field by 17.5 and 18 ppm in **4** and **6** compared to the free substrates, respectively. Even if a perturbation of the chemical shift is expected due to the alkyl binding to the metal, the size of the perturbation suggests a direct contact of the carboxyl moiety with the Ni. To prove this assumption theoretically, NMR chemical shift calculations were performed. The ^{13}C chemical shifts obtained for **4** with the B3LYP functional,[19,20] the 6-31g(d)[22] basis set for Ni, and the 6-311g(d)[23,24] basis set for all other atoms (parameters for iodine were obtained from the basis set exchange server[36,37]) are given in the supporting information (see Supporting Information Table S1). These calculations uncover a major discrepancy between theory and experiment for carbon atoms directly bound to the iodine. It is known from the literature that the influence of heavy elements on the chemical shift is difficult to predict.[38,39] For such a heavy nucleus relativistic effects already play a nonnegligible role. The use of effective-core potentials did not lead to an improvement (data not shown). Since good agreement for these carbons could not be achieved (inclusion of relativistic effects would lead to an unreasonable computational demand), we decided to replace the iodine by chlorine in all following calculations. In this way, we will still treat the electrostatic long-range influence of the halogenide in an approximate way but with a significant reduction in computer time.

Table 3. ^{13}C NMR chemical shifts for the α methoxycarbonyl ethyl ligand in **4** calculated using different functional and basis set combinations: The corresponding atoms are printed in italics and the atom numbers according to Figure 2 are given in brackets.

R=methyl acrylate	^{13}C NMR chemical shift				
		6 311G(d)		6 31G(d)	
Atoms	Experimental	B3LYP	BP86	B3LYP	BP86
Ni(II)—***C***$HCH_3C(O)OCH_3$ (2)	4.4	28.7278	46.8875	20.6532	39.4179
Ni(II)—CH***C***$H_3C(O)OCH_3$ (3)	15.6	15.1677	16.3515	14.5422	16.9235
Ni(II)—$CHCH_3$***C***$(O)OCH_3$ (4)	184.3	190.8374	185.1348	175.0061	170.7787
Ni(II)—$CHCH_3C(O)O$***C***H_3 (7)	51.3	52.5926	52.9502	49.9353	51.1354
Ni(II)—$P($***C***$H_3)_3$ (9 11)	12.5	16.7058	15.7713	13.5311	15.2489

The overall good agreement between experiment and calculation of the remaining nuclei (neglecting the carbon atoms bound to the halogenide) verifies that the geometries of the complexes obtained from the energy optimization are reasonable (see Supporting Information Table S1 as well as Tables 3 and 4 for the most important findings). Due to its slightly better performance, we will limit the discussion to the B3LYP functional and the 6-311g(d) basis set in the following.

Table 4. ^{13}C NMR chemical shifts for the α acetoxy ethyl ligand in **6** calculated using different functional and basis set combinations: The corresponding atoms are printed in italics and the atom numbers according to Figure 3 are given in brackets.

R=vinyl acetate	^{13}C NMR chemical shift				
		6 311G(d)		6 31G(d)	
Atoms	Experimental	B3LYP	BP86	B3LYP	BP86
Ni(II)—***C***$HCH_3O(O)CCH_3$ (2)	96.0	97.6021	108.3375	86.7619	98.6949
Ni(II)—CH***C***$H_3O(O)CCH_3$ (3)	n.d.	21.5935	21.6792	20.5702	21.5917
Ni(II)—$CHCH_3O(O)$***C***CH_3 (5)	186.4	176.7498	172.0462	163.8761	161.1084
Ni(II)—$CHCH_3O(O)C$***C***H_3 (7)	21.0	22.4989	20.6442	20.9081	20.0838
Ni(II)—$P($***C***$H_3)_3$ (9 11)	12.7	16.7828	17.8108	14.6992	16.6311

n.d.: Not detected.

Chemical shift of carbonyl group

As already mentioned, the primary goal of the calculation was to explain the large low-field shift of the $C_{carbonyl}$ chemical shift (184.3 ppm in **4** and 186.4 ppm in **6**) observed for both complexes. In the previous publication, this was reasoned by an interaction between $O_{carbonyl}$ and Ni. Our NMR calculations reproduce this low-field shift and even overestimate it for **4**. In contrast, the predicted chemical shift in **6** is in the range of an unperturbed carbonyl group. If the chemical shift perturbation was caused by the influence of Ni mediated through a Ni $O_{carbonyl}$ bond, one would have expected the same magnitude of the perturbation in both complexes, since the distances are very similar (3.095 and 3.035 Å for the **4** and **6**, respectively). To analyze this discrepancy between calculated and observed chemical shifts, additional relaxed potential energy surface scans were performed. In these calculations, one degree of freedom is varied between a minimum and a maximum value in discrete steps and all other variables are fully optimized for each of these steps. In the first scan, the distance between Ni and $O_{carbonyl}$ in **4** is increased from 3.095 (the optimal value) to 3.495 Å in 0.1 Å increments. For all these distances, the NMR chemical shift of $C_{carbonyl}$ only changes insignificantly showing always the extreme low-field shift (see Supporting Information Table S2). This demonstrates that weakening the Ni O interaction does not have an influence on the chemical shifts. The next possibility is that the chemical shift perturbation results from a direct 'through-space' interaction between Ni and $C_{carbonyl}$. To test this, the distance between these two atoms was reduced in **6** (from the optimized value of 3.268 to 2.568 Å in 0.1 Å increments) by fixing the distance at the corresponding value and optimizing all other degrees of freedom (relaxed potential energy scan). This led to an steady increase of the $C_{carbonyl}$ NMR chemical shift from 176.7 to 184.1 ppm almost reaching the experimental value of 186.4 ppm (see also Supporting Information Table S4). At the same time, the distance between $O_{carbonyl}$ and Ni shortens, so that similar effects can be obtained by artificially decreasing this distance (data not shown). Finally, the bond between the PMe_3 group and Ni is weakened as a result of the approaching carbonyl group resulting in a somewhat longer P Ni distance (2.268 Å compared to 2.243 Å in the optimized starting structure). It should be kept in mind that all our calculations are performed *in vacuo*. Solvent effects may also account for a weakening and a strengthening of the PMe_3 and $C_{carbonyl}$ coordination, respectively. Concluding these findings, the reasons for the low-field shift of the $C_{carbonyl}$ NMR chemical shift in the **6** can, in our opinion, still be seen in the interaction between $O_{carbonyl}$ and Ni. Even if the perturbation is most likely caused by the direct influence of Ni and not mediated through the oxygen, the short distance between Ni and $C_{carbonyl}$ is a result of the Ni O interaction.

As just mentioned, the Ni PMe_3 interaction becomes weaker if the Ni O bond is shortened. Thus, it is interesting if the same behavior can also be achieved by not strengthen the Ni O but weakening of the Ni P bond. A relaxed potential energy surface scan was performed for **6**, in which the length of the Ni P bond was increased from 2.238 to 2.938 Å again in 0.1 Å increments. In the first few steps of this scan, the Ni C and Ni O distance only shortens slightly. This is accompanied also by a minor change in the $C_{carbonyl}$ NMR chemical shift to 179.0 ppm at a Ni P distance of 2.738 Å (see Supporting Information Table S5). In this structure, the Ni O distance (2.739 Å) is approximately the same as the Ni P distance. In the following step, the geometry of the complex changes drastically. Especially, the Ni O distance is reduced to 1.954 Å and $O_{carbonyl}$ is now occupying the fourth position of the quadratic-planar arrangement around the Ni ion previously filled by the PMe_3 group (see Fig. 4). This shows that it is favorable for the α-acetoxy ethyl ligand to act as a chelate ligand building a five-membered ring. *In vacuo*, the abstraction of the PMe_3 group is associated with a high-energy barrier. But in the real system, the solvents will facilitate this process and rearrangement of the ligand shell around the Ni ion is more likely to occur. One can speculate that the rearrangement could result in a different coordination sphere having the phosphine in the fifth non-planar coordination position. This is supported by the chemical shift of $C_{carbonyl}$, which jumps to 187.5 ppm during ring formation being almost identical to the experimental value. To simulate the rebinding, the first structure of the energy scan showing the five-membered ring (Fig. 4) was optimized again without any constraints. This did not result in a rebinding of the phosphine but in a further increase in the Ni P distance from 2.838 to 4.126 Å (Fig. 4). Therefore, the rebinding is associated with a reaction barrier and had to be modeled by an additional relaxed potential energy scan, in which the Ni P distance was reduced to the length in the optimized starting structure (the one resulting from the reoptimization of the structures of the Berkefeld et al. publication[12]) of 2.238 Å. The geometry of the end conformation was exactly the same as in the optimized starting structure having the PMe_3 group as one ligand of the quadratic-planar arrangement around the Ni ion (Fig. 4), which demonstrates, in contrast to the speculation suggested above, that only the original coordination sphere is energetically accessible and that the low-field shifted NMR chemical shift of $C_{carbonyl}$ cannot be explained by the rearrangement of the coordination sphere. Nevertheless, due

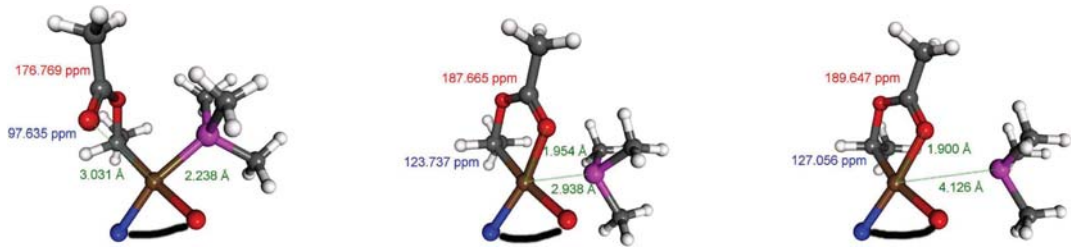

Figure 4. Structures resulting from the relaxed potential energy scans of **6**, in which the Ni—P bond length is stepwise increased (release scan) and decreased (rebinding scan), respectively. The distances from Ni to $O_{carbonyl}$ as well as to the directly bound carbon atom are shown in green. The chemical shift of $C_{carbonyl}$ and of the directly bound carbon atom are given in red and blue, respectively. For clarity, the (N,O) ligand is removed and only the coordinating N and O atoms are shown in the presentation. Left: optimized starting structure, which is indistinguishable from the end structure of the rebinding scan. Middle: first structure of release scan, in which the five membered ring is formed. Right: end structure of unconstrained optimization starting from structure shown in the middle [Color figure can be viewed in the online issue, which is available at wileyonlinelibrary.com.]

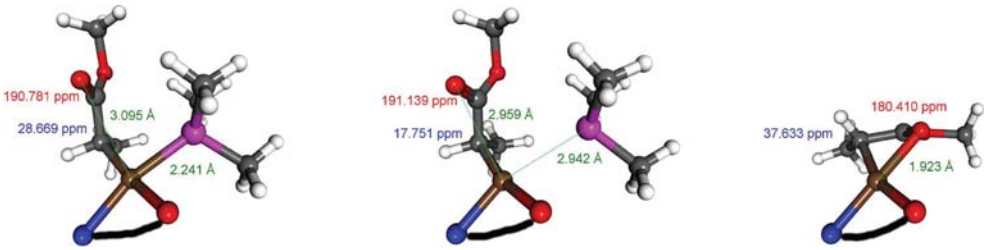

Figure 5. Structures resulting from the relaxed potential energy scans of **4**, in which the Ni—P bond length is stepwise increased. The distances from Ni to $O_{carbonyl}$ as well as to the directly bound carbon atom are shown in green. The chemical shift of $C_{carbonyl}$ and of the directly bound carbon atom are given in red and blue, respectively. For clarity, the (N,O) ligand is removed and only the coordinating N and O atoms are shown in the presentation. Left: optimized starting structure. Middle: end structure of the energy scan, where the Ni—P distance is increased to 2.942 Å. Right: structure in which the PMe_3 group is fully removed, showing the quadratic planar arrangement of the ligands [Color figure can be viewed in the online issue, which is available at wileyonlinelibrary.com.]

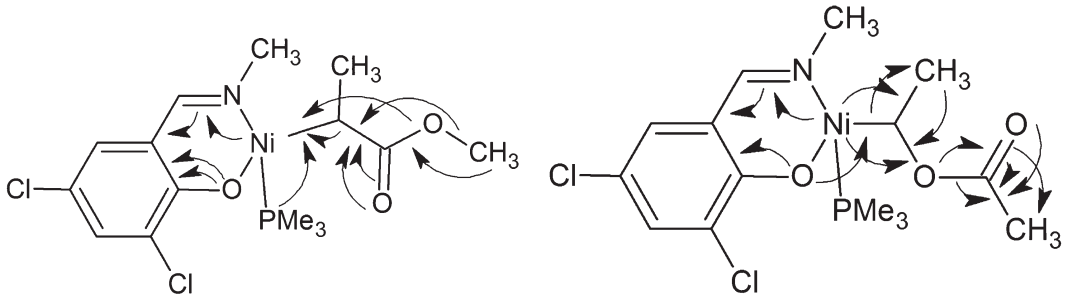

(a) Fragment of **4** (b) Fragment of **6**

Figure 6. Direction of the main electron shifts. The arrows point from the NBOs including lone pairs, from which electron density is removed, to the NBOs accepting the electron density. (Since the analysis starts from the Lewis structure shown, the main electron transfer from the N and O atoms of the (N,O) moiety forming the bonds to the Ni ion is not included and only the back donation from the Ni to the ligands is shown.)

to solvent effects not included in the calculations such a rearrangement might still be possible at least as a transient complex conformation.

The equivalent studies of **4** did not lead to the square planar arrangement with two coordination sites filled by the (N,O) ligand and the other two by the α-methoxycarbonyl ethyl ligand (C_1 and $O_{carboyl}$) even if the Ni P distance is increased to 2.942 Å (Fig. 5 and Supporting Information Table S3). Nevertheless, the Ni O distance is significantly shortened (from 3.095 Å in the optimized starting structure to 2.750 Å) indicating a strengthening of this interaction. Only if the phosphine is totally abstracted the chelate structure forms resulting in ring closure and the square planar orientation of the four ligands is formed. This late formation of the four-membered ring can be explained by the stronger conformational strain compared to the five-membered ring. These interactions

between Ni and $O_{carbonyl}$ might reduce the catalytic activity of the Ni(II) complex by a combination of electronic and steric effects as proposed by Berkefeld et al.[12] Even if $O_{carbonyl}$ is a weaker ligand than PMe_3 it is hindering the incorporation of a new monomer in this way contributing to the fact that the deactivation of the catalytic species is the dominant reaction path.

Coordinating carbon

The second region with remarkable effects of the complex formation on the NMR chemical shifts are the carbon atoms directly bound to Ni(II). For these atoms, chemical shifts of 4.4 and 96 ppm are detected in **4** and **6**, respectively (see Tables 3 and 4). These large differences become even more prominent if one compares these values with the chemical shifts in methyl propionate and ethyl acetate, which are the corresponding molecules if the metal fragment is replaced by a single hydrogen to analyze the influence of the metal. On the one hand, large changes are observed, which is not unexpected due to the perturbation of the electron density of the ligated atom caused by Ni(II). But, on the other hand, the chemical shifts change in opposite direction in these two complexes. While for **4** the chemical shift is shifted to higher field from 27.5[12]to 4.4 ppm, for **6** it is strongly down-field shifted from 60.4[12] to 96.0 ppm. The calculations reproduce the low-field shifted value of **6** perfectly. For **4**, the chemical shift is predicted as too large as shown in Table 3. To understand this behavior, NBO calculations were performed. Even though these give a very intuitive representation of the electron displacements in a molecule, they are difficult to analyze for large molecules. Therefore, different fragments of each complex were generated by removing parts of the terphenylamine moiety of the (N,O) ligand (see Supporting Information Figs. S1 and S2). For both complexes, the fragments, in which the two $(F_3C)_2C_6H_3$ substituents have been cut off (fragment 2, see Supporting Information Tables S5 and S6 and Fig. 6), were used for the further analysis since it is the smallest fragment still showing approximately the same geometrical arrangement as the full complex. Nevertheless, one should keep in mind that truncating a system may have detrimental influence on the results [46,47] and we, therefore, limit our discussion to a qualitative interpretation.

Beside the transformation of the molecular orbitals into localized orbitals, NBO also describes the electron distribution in these orbitals, that is, from which orbital electrons are transferred to other orbitals due to polarization effects in the molecule. The directions of the main electron displacements are shown in Figure 6. In **4**, the main electron shift is directed from the α-methoxycarbonyl ethyl ligand towards the region around the Ni ion. Thus, the electron density at Ni, and in this way also at the carbon, is increased due to this +I effect in **4** which results in the high-field perturbation (lower ppm value) of the ^{13}C chemical shift. This increased electron density is probably also a reason for the higher hydrolysis-sensitivity of **4** compared to other Ni-alkyl complexes, which are surprisingly resistant toward hydrolysis.[6] For the other complex, the electron transfer is exactly in the opposite direction from Ni(II) to $C_{carbonyl}$ and further on to the methyl group. Thus, the electron density is reduced around the Ni C bond, the nuclei are not so strongly shielded, and the ^{13}C resonance is observed at a lower field (high ppm values). Thus, the different influence of the Ni ion on the NMR chemical shift in **4** and **6** are reasonable described by the DFT calculations and can be explained by the different electronic polarizations in the two complexes. Only the over 20 ppm deviation between the computational and experimental value for the carbon directly bound to the Ni(II) of **4** is unsatisfying. Since additionally performed Møller–Plesset second-order perturbation theory (MP2) calculations on the fragment gave no significant improvements (see Supporting Information Fig. S3 and Table S8 for MP2 results on fragment 1), it seems that other effects than the level of theory, for example, polarization by the solvents, additional binding of solvent molecules (first shell solvent effects), and structural differences between the fragments and the full complex, have a much larger influence on the calculated chemical shifts causing the discrepancy between experiment and calculations. Additionally, one should keep in mind that NMR chemical shifts are properties of a thermodynamic ensemble at finite temperature and not of a single optimal structure. All these effect cannot be considered in the calculations with acceptable computational demand and, thus, no further investigations were performed.

Conclusions

Our DFT-based results are able to reproduce the correct trends of the ^{13}C NMR chemical shifts for Ni(II) complexes used as catalysts in olefin polymerization and to verify the structures proposed previously.[12] Nevertheless, they also show that the accurate calculation of the chemical shifts is not straight forward and that probably higher levels of theory combined with larger basis sets and inclusion of solvent effects (and relativistic effects) are needed to get an accuracy of less than 5 ppm for all carbons.[38–44] But even the qualitative description is very helpful to understand the electronic effects resulting from structural variations. Two such effects were analyzed in detail: (1) The low-field shift of the $C_{carbonyl}$ results from its close proximity to the Ni ion. Even if this short distance is enforced already by the first coordination of C_2 in **4**, an interaction between $O_{carbonyl}$ and Ni is needed in **6** to bring $C_{carbonyl}$ close to Ni. It is very likely and also confirmed by the previous[12] and our new calculations, that such an interaction is also present in **4** being a reason for the reduced reactivity. (2) The large difference in the chemical shifts of the carbon atoms directly coordinated to Ni could be explained by electron pushing and pulling effects on **4** and **6**, respectively. Thus, these chemical shifts can be used as very sensitive probe for the electrostatic properties around the Ni ion.

Acknowledgments

The authors thank Stefan Mecking for fruitful discussions and the careful reading of the manuscript. Additionally, the authors thank

the Common Ulm Stuttgart Server (CUSS) and the Baden-Württemberg grid (bwGRiD), which is part of the D-Grid system, for providing the computer resources making the computations possible.

Keywords: Ni(II) complexes · olefin polymerization · NMR chemical shifts · energy scans · natural bond orbitals

[1] S. D. Ittel, L. K. Johnson, M. Brookhart, *Chem. Rev.* **2000**, *100,* 1169.
[2] V. C. Gibson, S. K. Spitzmesser, *Chem. Rev.* **2002**, *103,* 283.
[3] S. Mecking, *Angew. Chem. Int. Ed.* **2001**, *40,* 534.
[4] E. Y. X. Chen, *Chem. Rev.* **2009**, *109,* 5127.
[5] A. Nakamura, S. Ito, K. Nozaki, *Chem. Rev.* **2009**, *109,* 5215.
[6] A. Berkefeld, S. Mecking, *Angew. Chem. Int. Ed.* **2008**, *47,* 2538.
[7] T. R. Younkin, E. F. Connor, J. I. Henderson, S. K. Friedrich, R. H. Grubbs, D. A. Bansleben, *Science* **2000**, *287,* 460.
[8] F. M. Bauers, S. Mecking, *Angew. Chem. Int. Ed.* **2001**, *40,* 3020.
[9] M. A. Zuideveld, P. Wehrmann, C. Rhr, S. Mecking, *Angew. Chem. Int. Ed.* **2004**, *43,* 869.
[10] I. Göttker Schnetmann, B. Korthals, S. Mecking, *J. Am. Chem. Soc.* **2006**, *128,* 7708.
[11] E. F. Connor, T. R. Younkin, J. I. Henderson, S. Hwang, R. H. Grubbs, W. P. Roberts, J. J. Litzau, *J. Polym. Sci. Part A* **2002**, *40,* 2842.
[12] A. Berkefeld, M. Drexler, H. M. Möller, S. Mecking, *J. Am. Chem. Soc.* **2009**, *131,* 12613.
[13] B. S. Williams, M. D. Leatherman, P. S. White, M. Brookhart, *J. Polym. Sci. Part A* **2002**, *40,* 2842.
[14] M. Brookhart, L. K. Johnson, C. M. Killian, L. Wang, Z. Y. Yang, *US Pat* **5880323**, 1999.
[15] Hyperchem (tm) (version 5), available at: www.hyper.com, Hypercube, Inc., 1115 NW 4th Street, Gainesville, Florida 32601, USA, Accessed on August 2008.
[16] Jaguar 5.5. Schrödinger, L.L.C., Portland, OR, **1991 2003**.
[17] M. J. Frisch, G. W. Trucks, H. B. Schlegel, G. E. Scuseria, M. A. Robb, J. R. Cheeseman, Jr., J. A. M., T. Vreven, K. N. Kudin, J. C. Burant, J. M. Millam, S. S. Iyengar, J. Tomasi, V. Barone, B. Mennucci, M. Cossi, G. Scalmani, N. Rega, G. A. Petersson, H. Nakatsuji, M. Hada, M. Ehara, K. Toyota, R. Fukuda, J. Hasegawa, M. Ishida, T. Nakajima, Y. Honda, O. Kitao, H. Nakai, M. Klene, X. Li, J. E. Knox, H. P. Hratchian, J. B. Cross, C. Adamo, J. Jaramillo, R. Gomperts, R. E. Stratmann, O. Yazyev, A. J. Austin, R. Cammi, C. Pomelli, J. W. Ochterski, P. Y. Ayala, K. Morokuma, G. A. Voth, P. Salvador, J. J. Dannenberg, V. G. Zakrzewski, S. Dapprich, A. D. Daniels, M. C. Strain, O. Farkas, D. K. Malick, A. D. Rabuck, K. Raghavachari, J. B. Foresman, J. V. Ortiz, Q. Cui, A. G. Baboul, S. Clifford, J. Cioslowski, B. B. Stefanov, G. Liu, A. Liashenko, P. Piskorz, I. Komaromi, R. L. Martin, D. J. Fox, T. Keith, M. A. Al Laham, C. Y. Peng, A. Nanayakkara, M. Challacombe, P. M. W. Gill, B. Johnson, W. Chen, M. W. Wong, C. Gonzalez, J. A. Pople, Gaussian 03, Revision C.02 Gaussian, Inc., Wallingford CT, USA, **2004**.
[18] J. P. Perdew,*Phys. Rev. B* **1986**, *33,* 8822.
[19] C. Lee, W. Yang, R. G. Parr, *Phys. Rev. B* **1988**, *37,* 785.
[20] B. Miehlich, A. Savin, H. Stoll, H. Preuss, *Chem. Phys. Lett.* **1989**, *157,* 200.
[21] R. Ditchfield, W. J. Hehre, J. A. Pople, *J. Chem. Phys.* **1971**, *54,* 724.
[22] V. A. Rassolov, J. A. Pople, M. A. Ratner, T. L. Windus, *J. Chem. Phys.* **1998**, *109,* 1223.
[23] A. D. McLean, G. S. Chandler, *J. Chem. Phys.* **1980**, *72,* 5639.
[24] R. Krishnan, J. S. Binkley, R. Seeger, J. A. Pople, *J. Chem. Phys.* **1980**, *72,* 650.
[25] F. London, *J. Phys. Radium* **1937**, *92,* 397.
[26] R. McWeeny, *Phys. Rev.* **1962**, *126,* 1028.
[27] R. Ditchfield, *Mol. Phys.* **1974**, *27,* 789.
[28] K. Wolinski, J. F. Hilton, P. Pulay, *J. Am. Chem. Soc.* **1990**, *112,* 8251.
[29] J. R. Cheeseman, G. W. Trucks, T. A. Keith, M. J. Frisch, *J. Chem. Phys.* **1996**, *104,* 5497.
[30] H. J. Reich, available at: http://www.chem.wisc.edu/∼nbo5/, **2007**, Accessed on December 2010.
[31] M. Head Gordon, J. A. Pople, M. J. Frisch, *Chem. Phys. Lett.* **1988**, *153,* 503.
[32] S. Saebø and J. Almlöf, *Chem. Phys. Lett.* **1989**, *154,* 83.
[33] M. J. Frisch, M. Head Gordon, J. A. Pople, *Chem. Phys. Lett.* **1990**, *166,* 275.
[34] M. J. Frisch, M. Head Gordon, J. A. Pople, *Chem. Phys. Lett.* **1990**, *166,* 281.
[35] M. Head Gordon, T. Head Gordon, *Chem. Phys. Lett.* **1994**, *220,* 122.
[36] D. Feller, *J. Comput. Chem.* **1996**, *17,* 1571.
[37] K. L. Schuchardt, B. T. Didier, T. Elsethagen, L. Sun, V. Gurumoorthi, J. Chase, J. Li, T. L. Windus, *J. Chem. Inf. Model* **2007**, *47,* 1045.
[38] L. B. Casabianca, A. C. de Dios, *J. Chem. Phys.* **2008**, *128,* 052201.
[39] T. Helgaker, M. Jaszuski, K. Ruud, *Chem. Rev.* **1999**, *99,* 293.
[40] A. Auer, J. Gauss, J. F. Stanton, *J. Chem. Phys.* **2003**, *118,* 10407.
[41] E. Prochnow, A. Auer, *J. Chem. Phys.* **2010**, *132,* 064109.
[42] T. H. Sefzik, D. Turco, R. J. Iuliucci, J. C. Facelli, *J. Phys. Chem. A* **2005**, *109,* 1180.
[43] T. Kupka, M. Stachow, M. Nieradka, J. Kaminsky, T. Pluta, *J. Chem. Theory Comput.* **2010**, *6,* 11580.
[44] J. N. Dumez, C. J. Pickard, *J. Chem. Phys.* **2009**, *130,* 104701.
[45] S. Mecking, A. Held, F. M. Bauers, *Angew. Chem. Int. Ed.* **2002**, *41,* 544.
[46] E. T. Diego Benitez, A. William, I. Goddard, *Organometallics* **2009**, *28*, 2646.
[47] Y. Zhao, D.G. Truhlar, *J. Chem. Theory Comput.* **2009**, *5*, 324.